Cellular and Molecular Neurobiology (2019) 39:769–782
https://doi.org/10.1007/s10571-019-00677-5

ORIGINAL RESEARCH

The Role Played by SLUG, an Epithelial–Mesenchymal Transition Factor, in Invasion and Therapeutic Resistance of Malignant Glioma

Se-Jeong Oh[1,2] · Eun-Jung Ahn[1,2] · Ok Kim[2] · Daru Kim[2] · Tae-Young Jung[1] · Shin Jung[1] · Jae-Hyuk Lee[2] · Kyung-Keun Kim[3] · Hangun Kim[4] · Eui Hyun Kim[5] · Kyung-Hwa Lee[2] · Kyung-Sub Moon[1]

Received: 31 October 2018 / Accepted: 16 April 2019 / Published online: 22 April 2019

Abstract

In malignant gliomas, invasive phenotype and cancer stemness promoting resurgence of residual tumor cells render treatment very difficult. Hence, identification of epithelial–mesenchymal transition (EMT) factors associated with invasion and stemness of glioma cells is critical. To address the issue, we investigated several EMT factors in hypermotile U87MG and U251 cells, orthotopic mouse glioma model, and human glioma samples. Of several EMT markers, SLUG expression was notably increased at the invasive fronts of gliomas, both in mouse tumor grafts and human glioma samples. The biological role played by SLUG was investigated using a colony-forming assay after chemotherapy and irradiation, and by employing a neurosphere culture assay. The effect of SLUG on glioma progression was examined in our patient cohort and samples, and compared to large public data from the REMBRANDT and TCGA. Genetic upregulation of SLUG was associated with increased levels of stemness factors and enhanced resistance to radiation and temozolomide. In our cohort, patients exhibiting lower-level SLUG expression evidenced longer progression-free survival ($P = 0.042$). Also, in the REMBRANDT dataset, a group in which SLUG was downregulated exhibited a significant survival benefit ($P < 0.001$). Although paired glioblastoma samples from our patients did not show a significant increase of SLUG expression, increased mRNA levels of SLUG were found in recurrent glioblastoma from TCGA ($P = 0.052$), and in temozolomide-treated glioma cells and mouse tumor grafts. SLUG may contribute to glioma progression by controlling invasion at infiltrating margins, associated with increased stemness and therapeutic resistance.

Keywords Cancer stem cell · Epithelial–mesenchymal transition · Malignant glioma · SLUG · Tumor progression

Abbreviations

E-Cad	E-cadherin
EMT	Epithelial–mesenchymal transition
FN	Fibronectin
IHC	Immunohistochemistry
N-Cad	N-cadherin
OS	Overall survival
PDX	Patient-derived xenograft
PBS	Phosphate-buffered saline
PFS	Progression-free survival
TMZ	Temozolomide
TCGA	The Cancer Genome Atlas

Electronic supplementary material The online version of this article (https://doi.org/10.1007/s10571-019-00677-5) contains supplementary material, which is available to authorized users.

✉ Kyung-Hwa Lee
mdkaylee@chonnam.ac.kr

✉ Kyung-Sub Moon
moonks@chonnam.ac.kr

Extended author information available on the last page of the article

Background

Glioblastoma is the most aggressive, common brain cancer and is difficult to treat. Generally, treatment includes surgery combined with adjuvant radiation and chemotherapy featuring alkylating agents. Despite major advances in treatment modalities, the survival of glioma patients remains poor. Gliomas are highly infiltrative; cells invade the surrounding normal brain tissue. Such invasiveness is the principal cause of poor outcomes and one of the major reasons for treatment failure. Despite the significance of invasion, the underlying mechanism remains obscure (Kleihues et al. 2007).

The fundamental feature of glioma invasion and therapeutic resistance may be the associated epithelial–mesenchymal transition (EMT) (Han et al. 2011; Mahabir et al. 2014; Mikheeva

et al. 2010; Xia et al. 2010; Yang et al. 2010). During the EMT, epithelial cells lose polarity, cell-to-cell adhesion ceases, and the cells acquire migratory, invasive mesenchymal phenotype (Gupta and Massague 2006; Peinado et al. 2007). The EMT thus facilitates cell motility and increases resistance to apoptosis (Kalluri and Neilson 2003). Suppression of the epithelial marker E-cadherin (E-Cad), coupled with activation of the mesenchymal marker N-cadherin (N-Cad), creates an aggressive phenotype promoting tumor progression; this process is termed the 'cadherin switch' (Cavallaro et al. 2002; Maeda et al. 2005). Recent studies found that the EMT promoted some stem cell properties in regular cancer cells (Mani et al. 2008; Polyak and Weinberg 2009) and drug resistance (Singh and Settleman 2010). Of the various EMT transcription factors, SNAI1, SLUG, Twist1, and/or ZEB1 confer stem cell-like properties on cancer cells (Dang et al. 2011; Mani et al. 2008; Wellner et al. 2009), which then engage in self-renewal and proliferation; these processes play crucial roles in fresh tumor initiation, growth, invasion, and recurrence.

SLUG is known to induce the EMT and to transcriptionally repress cell adhesion molecules (Barrallo-Gimeno and Nieto 2005; Nieto 2002). SLUG expression is associated with progressive tumor grades, lymph node metastasis, postoperative relapse, and poorer patient survival in several types of cancer (Shih et al. 2005; Shioiri et al. 2006; Uchikado et al. 2005). SLUG is found in the invasive fronts of tumors in which other epithelial genes encoding E-cadherin, occludin, ZO-1, and desmosomal junction components are suppressed (Cano et al. 2000; Kurrey et al. 2005; Savagner et al. 1997). SLUG indirectly activates mesenchymal genes including vimentin, N-Cad, and fibronectin (FN) (Nieto 2011). SLUG is well known to regulate the invasion of many cancers, including gastric, breast, lung, ovarian, and pancreatic cancer (Gonzalez and Medici 2014).

Here, we explored the roles played by various EMT factors in glioblastoma. We established hypermotile glioma cell lines using a repetitive scratch method and found that SLUG played a pivotal role in terms of frontal invasion. Although the roles played by SLUG in epithelial malignancies have been studied, this is not the case for malignant glioma. We focused on the biological roles of SLUG in glioblastoma patients from the viewpoints of stemness, invasiveness, and therapeutic resistance. Additionally, the clinical implications were investigated by analysis of relevant clinicopathological data including survival rates.

Materials and Methods

Cell Culture

Human glioma cells (the U87MG, U251, U118, T98G, and LN18 lines) were obtained from the American Type Culture Collection (Manassas, VA, USA). A mouse glioma cell line (GL261), originally developed by the NCI-Frederick Cancer Research Tumor Repository, was kindly provided by Prof. Maciej S. Lesniak (Northwestern University Feinberg School of Medicine, Chicago, IL, USA). Cells were cultured in Dulbecco's modified Eagle's medium (WELGENE, Gyeongsan-si, South Korea) supplemented with 10% (v/v) fetal bovine serum (FBS; WELGENE) in a humidified atmosphere with 5% (v/v) CO_2 at 37 °C.

Establishment of Hypermotile Cell

The method used to establish hypermotile glioma cell lines is summarized in Fig. 1a. U87MG cells were seeded in a 60-mm-diameter dish and cultured until confluent. A straight scratch was made in the center and cells below the wound were wiped away with a cotton swab. After cultured at 37° for 4 days, non-migrated cells within the wound were wiped away again and migrated cells were detached using trypsin–EDTA (GIBCO, Thermo Fisher Scientific, Waltham, MA, USA), and re-seeded, re-cultured, and re-wounded 10 times. Hypermotile U251 cells were established in the same manner.

Migration Assay

Cells were seeded in 96-well transparent tissue culture plates (ESSEN Bioscience, Ann Arbor, MI, USA) in 0.2 mL amounts of DMEM supplemented with 10% (v/v) FBS, and incubated for 24 h. Straight transverse lines were drawn through adherent cells using a 96-well woundmaker (ESSEN Bioscience), creating uniform gaps, and the plates were placed inside an IncuCyteTM (ESSEN Bioscience). Scans were scheduled every 2–4 h for 72 h, using ZOOM software (ESSEN Bioscience), and cell migration distances were measured. All assays were repeated three times.

Invasion Assay

Cell invasion was examined using Transwells with chambers separated by filters of 8 µm pore size (Corning Inc., Corning, NY, USA) according to the manufacturer's protocol. Briefly, 5×10^4 cells were seeded into the upper chamber in 120 µL amounts of medium containing 0.2% (w/v) bovine serum albumin (BSA). Then, 600 µL amounts of medium with 0.2% (w/v) BSA and 5 µg/mL human plasma FN (Calbiochem, San Diego, CA, USA) (a chemotactic factor) were added to the lower chamber. After 24 h of incubation, cells that had invaded the bottom surface of the Transwell were fixed, stained with Microscopy Hemacolor Rapid (a blood smear stain; Merck, Darmstadt, Germany) and counted in 3–5 fields under a light microscope. All assays were repeated three times.

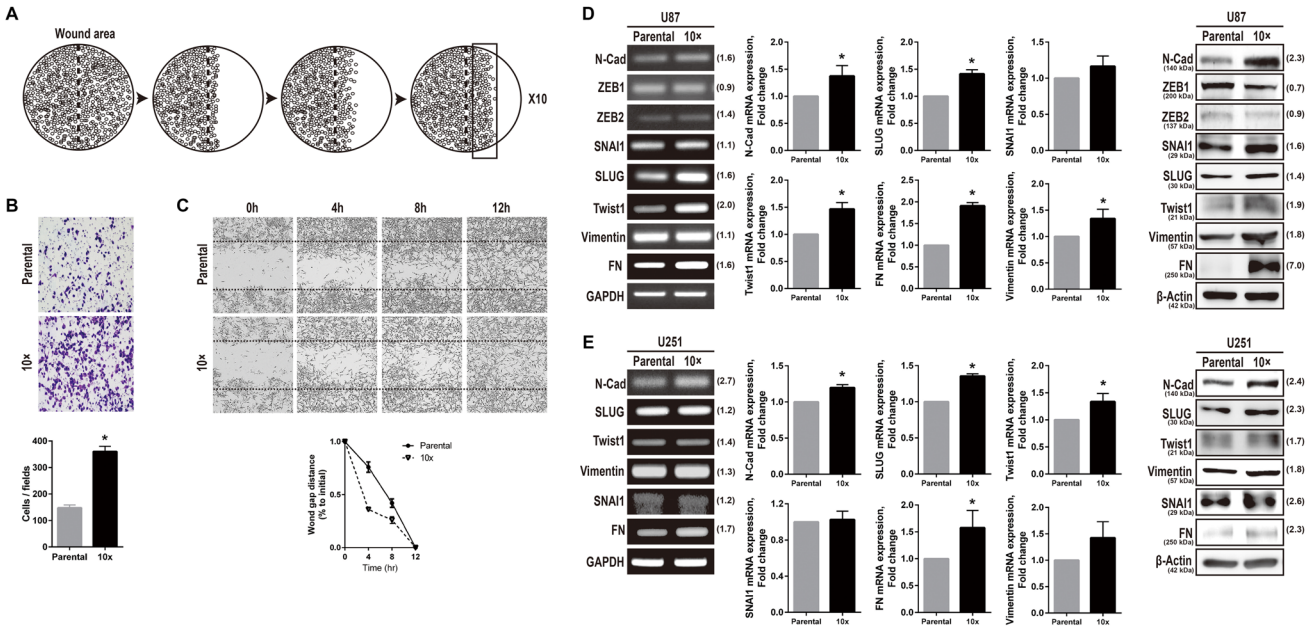

Fig. 1 Induction of EMT factors in hypermotile cells. **a** A schematic showing how hypermotile cell lines were established by a repeated scratch method. **b** Invasion assays were performed. The number of invading hypermotile cells was significantly greater than that of parental cells. **c** Migration assays were performed. Hypermotile cells exhibited a significant increase in migration capacity. Various EMT factors were induced in U87MG (**d**) and U251 (**e**) hypermotile cells. The expression levels increased at the mRNA level, as shown by RT-PCR (left panel) and qRT-PCR (middle panel), and at the protein level, as shown by Western blotting (right panel). GAPDH and beta-actin served as the internal normalization standards. The bar graphs show the mean ± SEM. The asterisk indicates a significant difference between the groups (*$P < 0.05$) (*N-Cad* N-cadherin, *FN* fibronectin)

RT-PCR and Real-Time PCR

Total RNA was prepared using the TRIzol reagent (Takara, Mountain View, CA, USA). 1 μg amounts of total RNA were transcribed to cDNA using random primers in a reaction volume of 20 μL. PCR amplification of cDNA was performed using gene-specific primers under the following conditions: denaturation at 95 °C for 15 min, followed by 35 cycles of denaturation at 95 °C for 30 s, annealing at 60 °C for 30 s, extension at 72 °C for 30 s, and a final extension at 72 °C for 5 min. PCR products were electrophoresed in agarose gels containing ethidium bromide and visualized using a Gel Doc EZ imager (Bio-Rad Laboratories, Hercules, CA, USA).

mRNA levels were quantified by real-time PCR using VeriQuest SYBR Green qPCR Master Mix (Affymetrix Inc, Santa Clara, CA, USA) and an Applied Biotech (Austin, TX, USA) platform. Real-time PCR and data collection were performed using a CFX 96 Touch Real-time PCR Detection System running CFX Manager software (Bio-Rad Laboratories) under the following conditions: hot start at 95 °C for 10 min, followed by denaturation at 95 °C for 15 s, annealing at 60 °C for 30 s, and elongation at 72 °C for 30 s (40 cycles). The relative levels of tested genes were normalized to those of an endogenous control (GAPDH) using the comparative 2-ΔΔ method. All real-time PCR assays were repeated three times. The primer sequences used are listed in Electronic Supplementary Table 1.

Western Blotting

Total cellular proteins were extracted into RIPA buffer (Bio Solution, Seoul, South Korea) supplemented with a protease inhibitor cocktail (Roche, Mannheim, Germany). Briefly, lysates were cleared by centrifugation and supernatants containing proteins collected for immunoblotting. Extracted proteins (20–40 μg) were electroblotted onto polyvinylidene fluoride (PVDF) membranes (GE Healthcare Life Science, Marlborough, MA, USA), probed with primary antibodies overnight, and incubated with horseradish peroxidase (HRP)-conjugated anti-mouse or anti-rabbit secondary antibodies; bands were detected using an electrochemiluminescence (ECL) system (Millipore, Burlington, MA, USA). The bands were quantitated with the aid of a LAS-4000 luminescent image analyzer (Fujifilm, Tokyo, Japan). The primary and secondary antibodies used are listed in Electronic Supplementary Table 2.

Glioma Patients and Tissue Specimens

Glioma specimens ($n = 92$) were obtained from patients who underwent surgical resection at Chonnam National University Hwasun Hospital between 2007 and 2012. The World Health Organization (WHO) Central Nervous System Classification in 2007 was used for diagnosis (Kleihues et al. 2007). Clinicopathological data were retrieved from medical records. Overall survival (OS) and progression-free survival (PFS) were determined as previously described (Lee et al. 2015). The clinical and radiological data of enrolled patients are summarized in Electronic Supplementary Table 3. Four matched pairs of primary and recurrent glioblastomas from the same patients were used for RNA analysis. The primary tumors were treated with the standard protocol including concurrent radiotherapy and temozolomide (TMZ) treatment, followed by adjuvant TMZ. Fresh frozen tissues were processed for RNA extraction analysis as previously described (Kwon et al. 2015). The analysis of microarray data was commissioned by Theragen Etex Bio Institute (Suwon, Korea). All data processing was performed using the R/Bioconductor packages and the p value was calculated using the limma package (ver.3.5.0, http://www.bioconductor.org). The Chonnam National University Hwasun Hospital Institutional Review Board approved this study (CNUHH-2016-081); we obtained written informed consent from patients or their legal surrogates for our use of resected glioma samples.

Tissue Microarray Construction and Immunohistochemistry

Areas of high cellularity were selected for microarray analysis. Tissue microarray construction and immunohistochemical staining were performed as described previously (Lee et al. 2015). The following antibodies were used for immunohistochemistry (IHC): anti-SLUG (dilution 1:100, catalog no. 9585; Cell Signaling, Boston, MA, USA); anti-Twist1 (dilution 1:100, ab-50887; Abcam, Cambridge, UK); and anti-SNAI1 (dilution 1:100, sc-28199; Santa Cruz Biotechnology, Dallas, TX, USA), with the aid of a Bond-Max Autostainer system (Leica Microsystems, Buffalo Grove, IL, USA). All immunostained slides were evaluated twice by experienced pathologists (LJH and LKH) blinded to the clinical details. The intensity of staining was initially classified into four grades: 0, no immunoreaction; 1, weak positivity; 2, moderate positivity; and 3, strong reactivity. Cases of grades 0 and 1 were categorized as low-expression cases, and cases of grades 2 and 3 as high-expression cases.

Patient Datasets of REMBRANDT and TCGA and Data Analysis

The database of the earlier NCI REMBRANDT (formerly at https://caintegrator.nci.nih.gov/rembrandt/login.do, but currently housed in the Georgetown University G-DOC System) contains de-identified open-access data on 343 glioma patients treated through May 13, 2014. We explored correlations between EMT factor expression levels and OS, as described previously (Noh et al. 2017). Graphs were constructed by comparing data from the Affymetrix reporter 219330 at the Highest Geometric Mean Intensity and related survival. The upregulated, downregulated, and intermediate groups all exhibited changes ≥ twofold in EMT factor levels compared to those of non-glioma samples. Survival differences among groups were compared using the log-rank test.

Gene expression data (Illumina HiSeq 2000 RNA Sequencing platform) of 172 glioblastoma samples from The Cancer Genome Atlas (TCGA) project were obtained from the data portal site (https://tcga-data.nci.nih.gov). Gene expression data were re-normalized before analysis. After exclusion of 5 normal brain samples, the expression level of SLUG was compared between 154 primary and 13 recurrent glioblastoma samples. Statistical analyses were performed in the R language (http://www.r-project.org). A P value < 0.05 was considered statistically significant unless otherwise indicated.

Plasmid and Lentiviral Infection of Target Cells

To overexpress SLUG, the full-length human SLUG gene was cloned by RT-PCR from U87MG cells using the slug-*Eco*R1 forward primer 5′-TTGAATTCATGCCGCGCTCCT TCCTGG-3′ and the slug-*BamH*1 reverse primer 5′-CCG GATCCTCAGTGTGCTACACAGCA-3′. The initial step was 3 min at 95 °C, followed by 35 cycles of 30 s at 95 °C, 1 min at 60 °C, and 2 min at 72 °C; the final polymerization was performed over 5 min at 72 °C. The amplicon was cloned into the pLVX-IRES-ZsGreen1 vector (Clontech Laboratories, Mountain View, CA, USA) digested with the enzymes indicated above. The accuracy of the SLUG sequence was confirmed by direct DNA sequencing. 293T cells were cultured and transfected with 16 μg plasmid DNA or DMEM-only (control). Virus samples were collected 48 and 72 h after transfection and concentrated via ultracentrifugation (Beckman Coulter, Brea, CA, USA).

For SLUG knockdown, we used the pSUPER RNAi System (Oligoengine, Seattle, WA, USA) and the *Bgl*II/*Xho*I oligonucleotides of the pSUPER vector. The cloning primers were sense, 5′-GAGAGAATAAAAGACAGTA-3′ and antisense, 5′-TACTGTCTTTTATTCTCTC-3′, in line with the manufacturer's protocol. Briefly, the two DNA oligonucleotides were incubated to facilitate RNA hairpin expression,

ligated into the pSUPER vector, and transformed into bacteria. The correct SLUG sequence was confirmed via direct DNA sequencing and stable pSUPER-sh-SLUG-expressing cell lines were selected using neomycin.

For lentiviral infection, cells were plated into 6-well plates at a multiplicity of infection, incubated overnight, and growth was allowed to continue for 48 h after addition of fresh growth medium. SLUG expression was confirmed at both the mRNA and protein levels.

Colony-Forming Assay

Equal numbers of glioma cells were grown in 6-well plates at a clonogenic density and were irradiated using a Gammacell 1000 instrument (Best Theratronics, Ottawa, Canada) at the indicated doses. After 9–14 days of incubation, the medium was discarded and the colonies were fixed in methyl alcohol followed by staining with crystal violet (Sigma–Aldrich, St. Louis, MO, USA). Only colonies containing > 25–50 cells were selected. To explore chemoresistance, the cells were plated, cultured overnight, and treated with 300, 500, and 700 μM TMZ for 48 h. Then, the culture medium was replaced by drug-free medium and the plates incubated for 14 days. TMZ was the kind gift of MSD Korea Ltd. (Seoul, South Korea) and was dissolved in dimethyl sulfoxide (Sigma–Aldrich).

Neurosphere Culture

Cells were plated and grown for 2 days in complete DMEM supplemented with 10% (v/v) FBS, washed, and replated at 1×10^4 cells/mL in T-25 flasks. The neurosphere culture medium was Neurobasal Medium (Thermo Fisher Scientific), supplemented with B27 (Thermo Fisher Scientific), 50 ng/mL epidermal growth factor and 50 ng/mL fibroblast growth factor (BD Biosciences, Franklin Lakes, NJ, USA), and 500 μM L-glutamine (Lonza, Basel, Switzerland). The flasks were placed in a CO_2 incubator for 7 days; the cells were collected and subjected to mechanical dissociation and viable cells were counted using the Trypan blue exclusion assay. As a secondary assay, viable cells were resuspended in proliferation medium, plated at 2×10^4 cells/mL in wells of a T-25 flask, and allowed to form neurospheres for 14 days; then, neurosphere numbers were microscopically counted.

Mouse Orthotopic Intracranial Glioma Model

Six-to-seven-week-old male C57BL/6 mice were purchased from OrientBio (Seongnam, South Korea) and maintained in an animal house with free access to autoclaved pelleted food and water. The experimental protocol was approved by the Chonnam National University Medical School Research Institutional Animal Care and Use Committee. Animal maintenance and all in vivo experiments were performed according to the Guiding Principles for the Care and Use of Animals (DHEW publication, NIH 80-23). Prior to intracranial injection, the mice were anesthetized and burr holes 1 mm in diameter were created in the right hemispheres, through which GL261 cells were injected using a 26-gauge Hamilton syringe (Hamilton Company, Reno, NV, USA) to a depth of 3 mm. Tumor-bearing mice were euthanized via cervical dislocation and the brains were extracted and fixed in 10% (v/v) neutral-buffered formalin for 3 days. The brains were dissected, embedded in paraffin, and stained with hematoxylin and eosin for histopathological evaluation. Brain samples of BALB/c nude mice implanted with human glioma cells (U87MG, U251, and U343) and patient-derived glioblastoma cells (GBM No. 11-15) were kindly supplied by Dr. Chung-Kwon Kim (Sungkyunkwan University, Suwon, South Korea) and Prof. Seok-Gu Kang (Yonsei University, Seoul, South Korea).

Statistical Analysis

All data were analyzed using IBM SPSS Statistics for Windows software (ver. 23.0; IBM Corp., Armonk, NY, USA). To compare EMT factor expression levels and WHO tumor grades, we employed the χ^2 test or Fisher's exact probability test. The effects of single variables on OS or PFS were estimated by univariate analysis. Data are presented as mean ± standard deviation (SD) unless otherwise indicated; at least three independent experiments were performed. Unless stated otherwise, the t-test was used to compare groups. GraphPad Prism for Windows software (ver. 6.00; GraphPad, La Jolla, CA, USA) was employed to analyze in vitro data, presented as mean ± standard error of the mean (SEM). A p value < 0.05 was considered to reflect statistical significance.

Results

Induction of EMT Markers and Regulators in Established Hypermotile Cells

Hypermotile glioma cell lines were established using a repetitive scratch method (Fig. 1a). Transwell invasion and wound-healing migration assays showed that the invasion and migration capacities of these cells were significantly increased compared to the parental cells (Fig. 1b, c). To investigate the factors associated with the invasion and migration of hypermotile cells, the expression levels of EMT markers and regulatory genes were investigated. In hypermotile U87MG cells, the expression of N-Cad, SLUG, Twist1, vimentin, and FN increased at both the mRNA and protein levels compared with the parental U87MG

cells (Fig. 1d). In hypermotile U251 cells, the expression of N-Cad, SLUG, Twist1, and FN increased compared to the parental cells (Fig. 1e). Although there have been some discrepancies between cell lines or between the analyzing methods, the overall directions of expression change showed that expression of EMT markers and inducers increased in both hypermotile cell lines.

SLUG Selected as EMT Regulator for Glioma Invasion in the Mouse Model and Human Sample

We used IHC to examine SLUG, SNAI1, and Twist1 expression in GL261-implanted mouse brains. Although all three EMT regulators were strongly expressed at the tumor margins (invasion fronts), the difference in expression intensity between the tumor center and the peripheral margin was more pronounced for SLUG compared to SNAI1 or Twist1 (Fig. 2a). High expression of SLUG in the peripheral margin of the tumor was found consistently (Electronic Supplementary Fig. 1). Thus, SLUG was a candidate EMT regulator during glioma invasion. In mouse xenograft models using human glioma cell lines and patient-derived glioblastoma cells, SLUG expression was again elevated in the tumor margins compared to the tumor centers (Fig. 2b). In tissue samples from glioblastoma patients, infiltrating tumor cells frequently exhibited similar SLUG expression differences between the tumor centers and the infiltrating margins (Fig. 2c). Thus, among the various EMT factors, SLUG appeared to play an important role in tumor invasiveness.

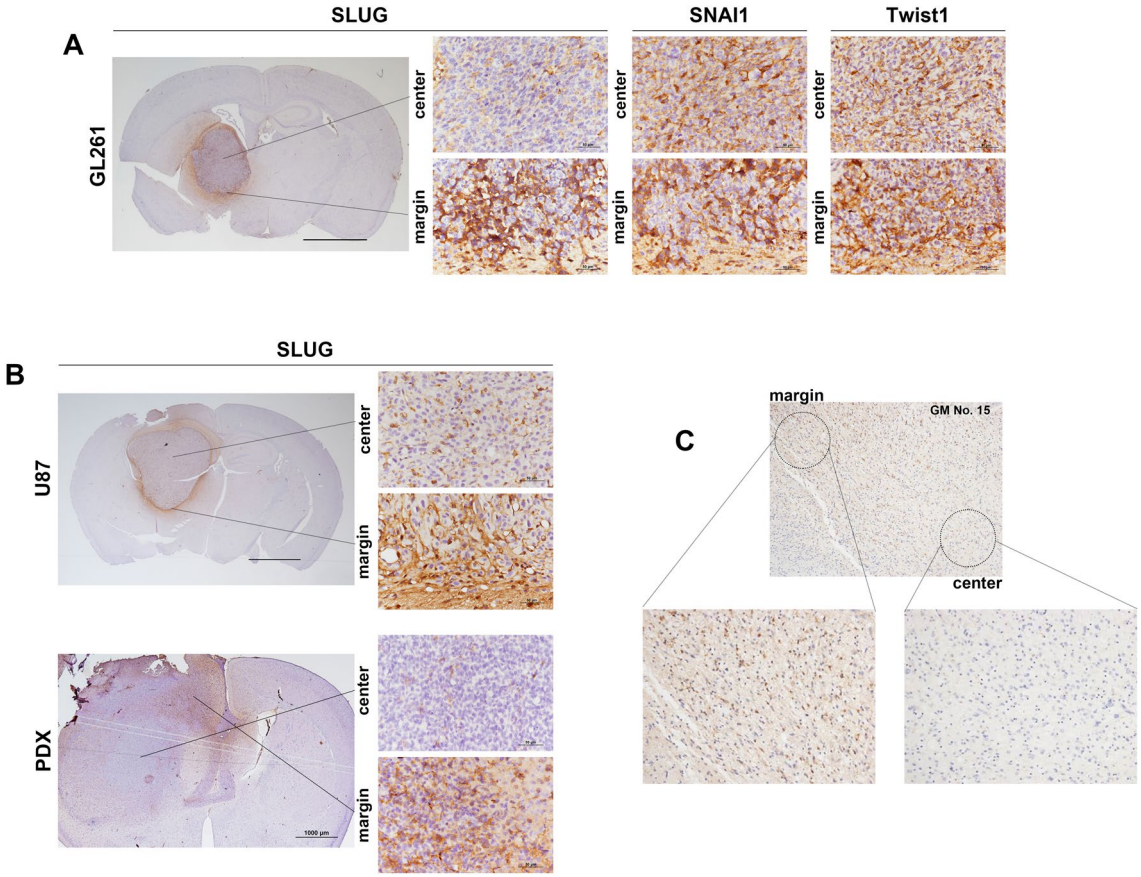

Fig. 2 SLUG expression in invasion fronts of the mouse model and the human sample. **a** Mouse GL261-implanted brain showed the prominent differential expression of SLUG, i.e., stronger expression in the invasion margins than in the center of the tumor. In comparison, the expression gap of SNAI1 or Twist1 was not remarkable (immunohistochemistry, original magnification × 400). **b** High-level SLUG expression was also evident in the marginal portions of mouse xenografts of human glioma cell lines. More interestingly, in the glioblastoma patient-derived xenograft (PDX) model, SLUG expression was higher in the invasion front of the corpus callosum than in the central portion (immunohistochemistry, original magnification × 400). **c** Glioblastoma tumor cells in the invading areas of patient tissue samples frequently expressed SLUG more strongly than did the central areas (immunohistochemistry, original magnification × 100 and × 200)

Invasion of Human Glioma Cells was Affected by Genetic Modulation of SLUG Expression

To determine whether the genetic modulation of SLUG expression affected invasion by human glioma cells, we created SLUG-overexpressing U87MG and U118 glioma cells using a pLVX-IRES-zsGreen1 lentivirus system (Fig. 3a). Cells overexpressing SLUG exhibited significantly more invasion than did cells with the empty IRES-SLUG vector (Fig. 3b). To explore how endogenous SLUG affected invasion, SLUG was knocked-down in U87MG cells using the pSUPER RNAi System (Fig. 3c). After the knockdown, the number of shSLUG-U87MG cells invading through the matrix decreased significantly compared to control cells (Fig. 3d). We also explored the associations between genetic SLUG modulation and the expression of other EMT factors. When SLUG was stably overexpressed in U87MG and U118 cells, the expression levels of N-Cad, Twist1, SNAI1, and FN increased significantly at both the protein and mRNA levels compared to control cells. On the contrary, on stable SLUG knockdown in U87MG cells, the expression of N-Cad, Twist1, SNAIl, and FN decreased significantly (Fig. 3e).

Increased Neurosphere-Forming Capacity and Expression of Stemness Markers in SLUG-Overexpressing Human Glioma Cells and Hypermotile Cells

To explore whether SLUG upregulation increased stemness, the neurosphere-forming capacity and levels of various stemness markers were measured in SLUG-overexpressing cell lines and hypermotile cells. Sphere-forming ability increased in U87MG and U118 cells overexpressing SLUG compared to control cells. Also, the levels of Msi, Bmi, CD44, and HES1 increased at the mRNA level in U118 cells overexpressing SLUG (Fig. 4a, b). Hypermotile cells also exhibited an enhanced sphere-forming ability compared to parental cells. The levels of mRNAs encoding ALDH1, Eph-B1, CD44, CD133, Msi, and HES1 were increased in hypermotile U87MG cells compared to parental cells (Electronic Supplementary Fig. 2). Together, the data showed that SLUG upregulation enhanced stem cell-like features at the invasive front of malignant glioma.

Therapeutic Resistance After Genetic Modulation of SLUG Expression in Human Glioma Cells

To explore the clinical implications of increased SLUG expression at tumor margins, we evaluated susceptibility to chemoradiation. After irradiation, the colony-forming assay showed that SLUG overexpression increased the survival of U87MG cells compared to controls. In contrast, after stable SLUG knockdown in U87MG cells, irradiation reduced the colony-forming capacity (Fig. 4c). We also explored whether SLUG overexpression promoted chemoresistance to TMZ of U87MG cells. SLUG-overexpressing cells exhibited a slightly higher colony-forming capacity than control cells (Fig. 4d). Together, the findings suggested that SLUG may increase therapeutic resistance during glioma treatment.

Clinical Effects of SLUG on Survival, Recurrence, and Therapeutic Resistance

IHC for SLUG was performed on TMA samples from 92 glioma patients. High-intensity SLUG staining was often evident in those with high-grade glioma ($P = 0.044$) (Electronic Supplementary Table 4). The median OS was 44.8 months [95% confidence interval (CI): 37.8–51.8 months]. However, the OS of patients expressing low levels of SLUG did not differ significantly ($P = 0.392$). In terms of PFS, the group expressing low-level SLUG showed a significant survival benefit compared to the high-level group ($P = 0.042$). In the 343 glioma patients of the REMBRANDT dataset, differences in SLUG expression were associated with significant variations in OS. SLUG upregulation, downregulation, or intermediate-level expression was associated with significant survival differences ($P < 0.001$) (Fig. 5a). In patients exhibiting high-level SLUG expression, OS was significantly curtailed.

RNA data of the matched pairs of glioblastoma samples showed that the expression of SLUG was higher in recurrent tumors treated with TMZ than in primary tumors, although there was no statistically significant difference ($P = 0.223$). In TCGA data, recurrent glioblastoma showed a significant increase of SLUG expression compared to initial resected glioblastoma, even though the samples were non-matched pairs ($P = 0.052$) (Fig. 5b). Thus, SLUG may impart resistance to glioblastoma treatment. The TMZ-resistance of T98G and LN18 glioma cells is attributable to long-term exposure to TMZ (Electronic Supplementary Fig. 3A). TMZ-resistant glioma cells exhibited increased SLUG expression at both the protein and mRNA levels (Fig. 5c). SLUG expression by TMZ exposure status was also examined in vivo (Electronic Supplementary Fig. 3B). Although TMZ initially suppressed tumor growth, all mice with GL261 implantation eventually died from tumor progression. SLUG expression in the central tumor regions increased in TMZ-treated mice compared to phosphate-buffered saline (PBS)-treated controls (Fig. 5d). Together, the data showed that SLUG expression was associated with TMZ-resistance, triggering tumor recurrence and poor outcomes in glioblastoma patients.

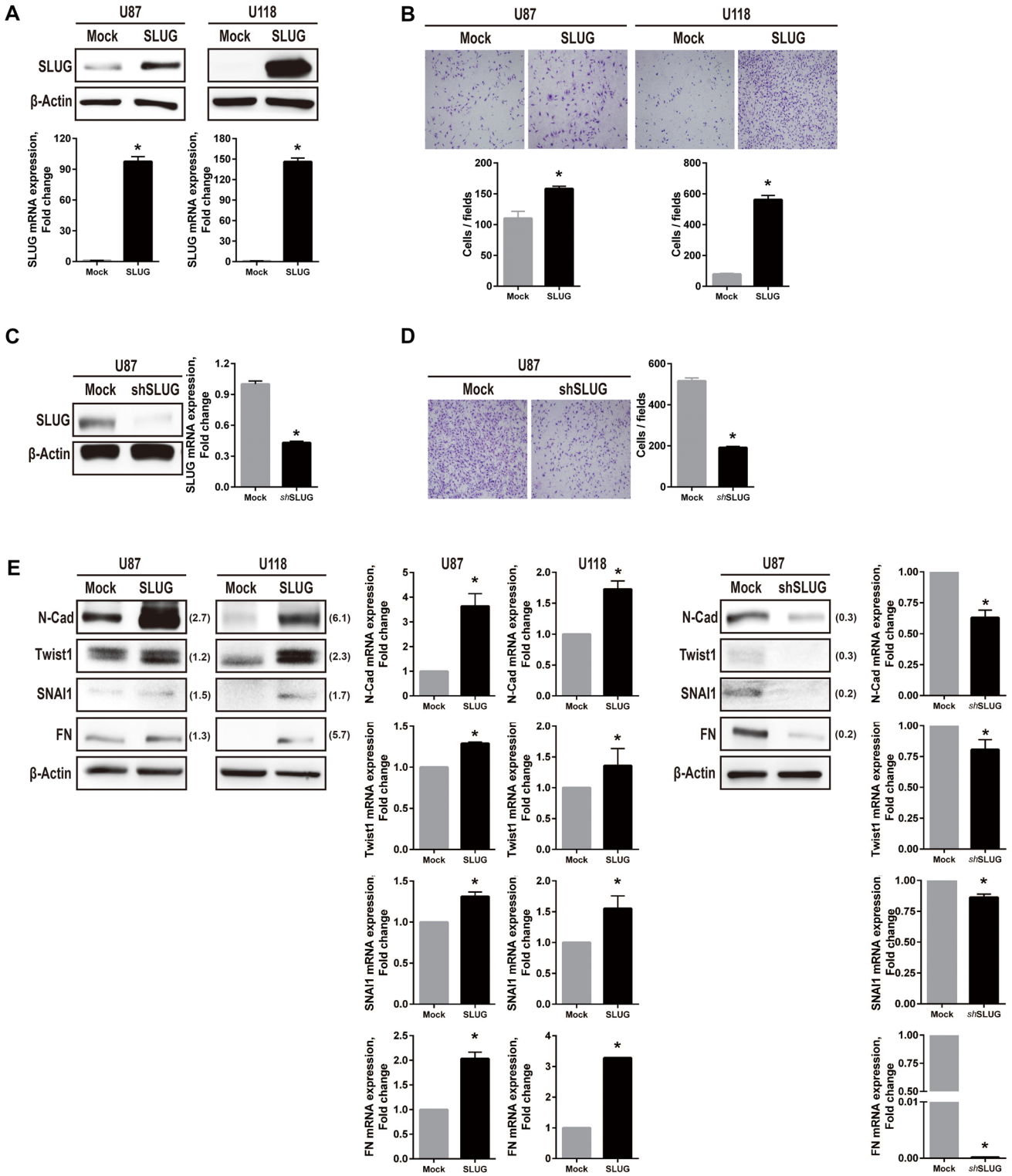

Fig. 3 Changes in glioma invasiveness by genetic modification of SLUG. **a** Western blotting and qRT-PCR analysis confirmed stable SLUG overexpression in the U87MG and U118 backgrounds. **b** In the invasion assay, cell infiltration was increased in U87 and U118 cell lines as a result of SLUG overexpression. **c**, **d** U87MG cells featuring stable SLUG knockdown were significantly less invasive than controls. **e** On stable overexpression of SLUG in U87MG and U118 cells, the expression levels of N-Cad, Twist1, SNAI1, and FN increased at the protein level, as shown by Western blotting; and at the mRNA level, as shown by qRT-PCR (left two panels). On the contrary, SLUG knockdown reduced EMT factor expression (right two panels). The bar graphs show the mean ± SEM. The asterisk indicates a significant difference between the groups (*$P < 0.05$) *N-Cad* N-cadherin, *FN* fibronectin

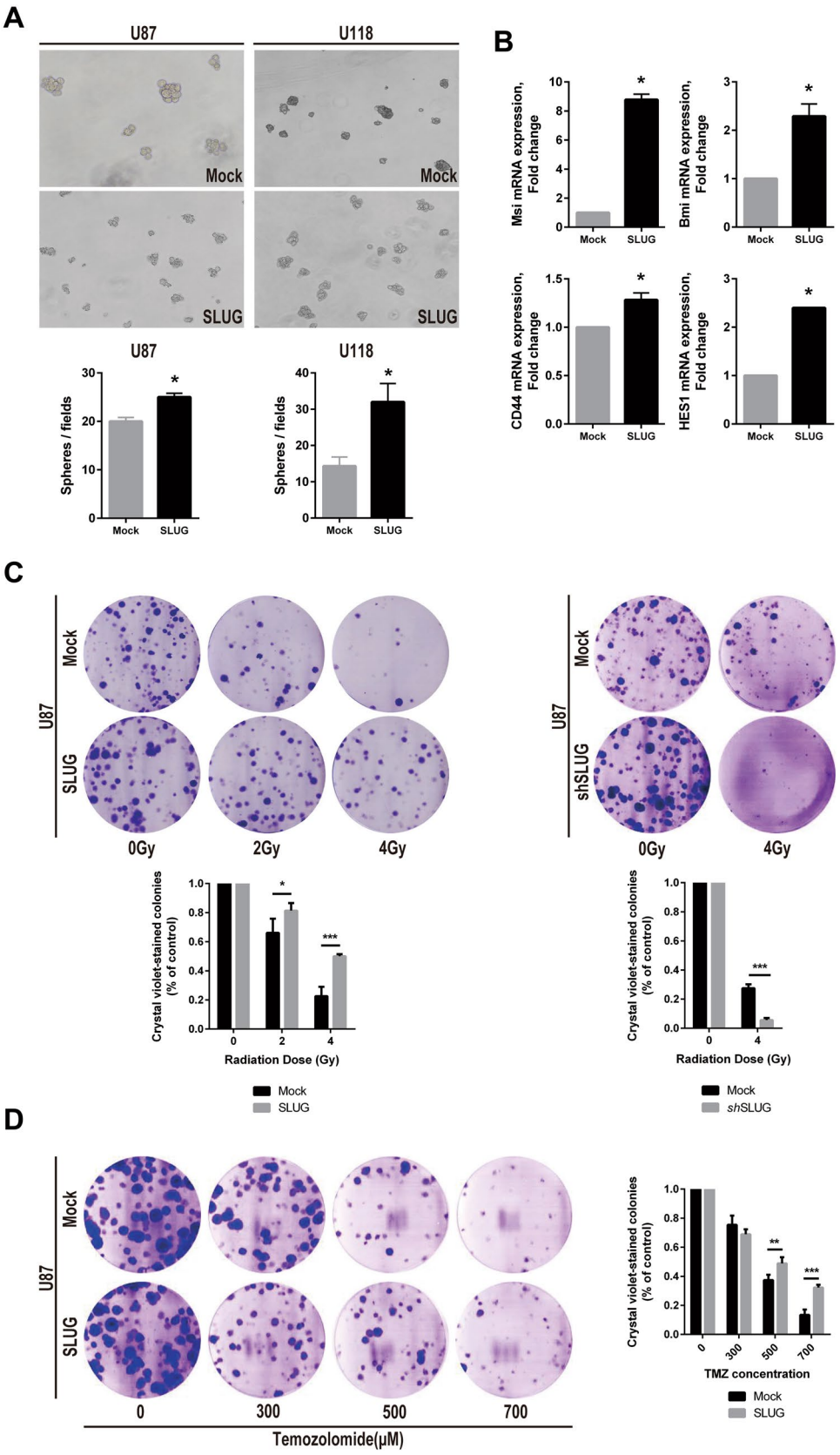

Fig. 4 Increased glioma stemness and therapeutic resistance by genetic modification of SLUG. **a** In the neurosphere culture assay, the number of neurospheres increased in SLUG-overexpressing cells compared to control. **b** In U118 glioma cells overexpressing SLUG, the qRT-PCR analysis revealed increased expression of stemness markers including Msi, Bmi, CD44, and HES1. **c** In the colony-forming assay, the SLUG-overexpressing cell was more radioresistant than the control and showed more colony counts. SLUG-knockdown cells exhibited significantly less colony formation and were more radiosensitive than control cells. **d** After TMZ treatment, U87MG cells featuring SLUG overexpression exhibited slightly more chemoresistance than control cells. Bar graphs show the mean ± SEM. The asterisks indicate significant differences between groups (*$P < 0.05$; **$P < 0.01$; ***$P < 0.001$)

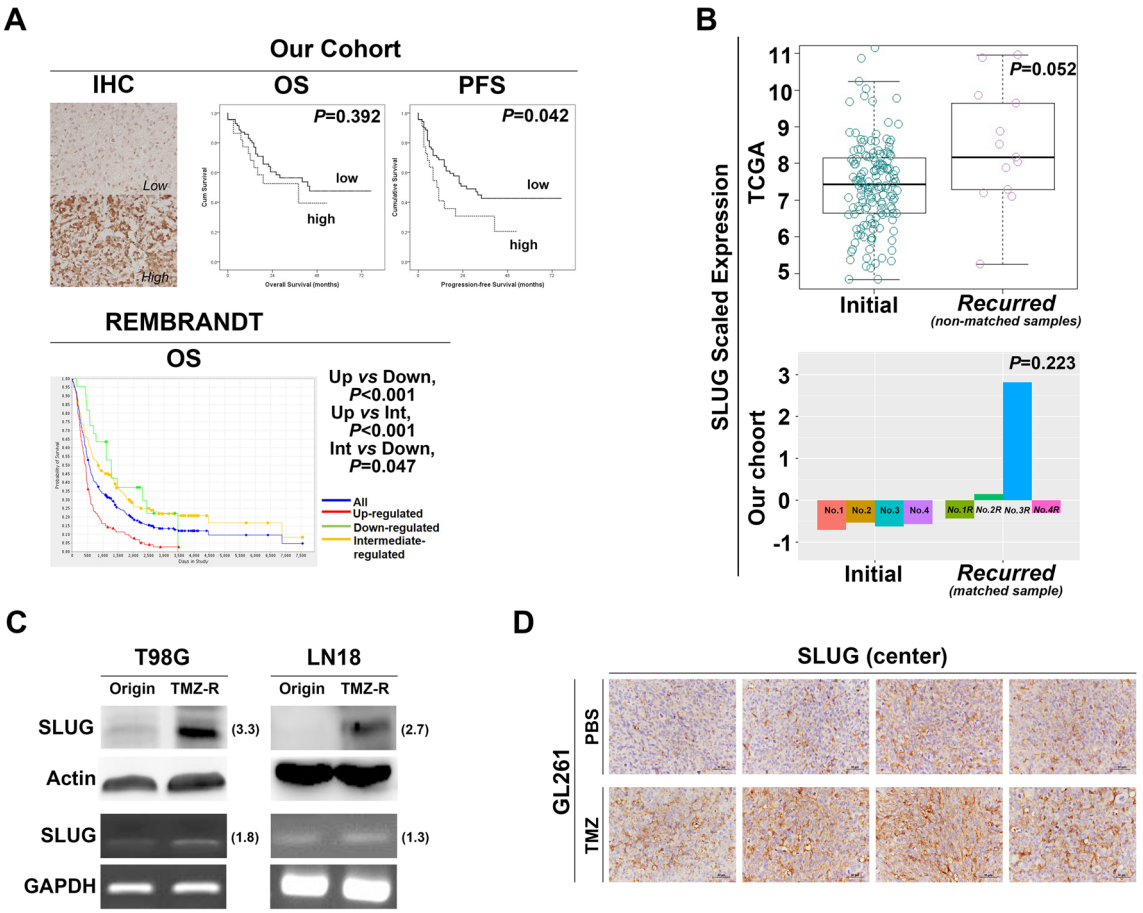

Fig. 5 The clinical significance of SLUG in terms of survival, recurrence, and therapeutic resistance. **a** In our cohort (92 glioma patients), SLUG significantly affected progression-free survival (PFS) ($P=0.042$), but not overall survival (OS) ($P=0.392$). In the REMBRANDT cohort ($n=343$), the levels of mRNA encoding SLUG correlated significantly with the OS gaps ($P<0.001$). **b** RNA data from TCGA [non-matched primary ($n=154$) vs. recurrent ($n=13$) glioblastoma] and our cohort (matched primary vs. recurrent glioblastoma, $n=4$) revealed that recurrent glioblastoma cases exhibited increased SLUG expression. **c** After long-term exposure to temozolomide (TMZ), SLUG expression increased in TMZ-resistant glioma cells, which was shown by Western blot at the protein level and by RT-PCR at the gene level. **d** In the GL261-implanted mouse model, SLUG expression increased in TMZ-treated mice compared to phosphate-buffered saline (PBS)-treated controls (immunohistochemistry, original magnification × 400)

Discussion

Invasive cancer phenotypes are closely linked to the actions of intracellular signaling pathways. EMT-activating transcription factors promote invasion and metastasis in an organized tumor-specific manner (Gonzalez and Medici 2014; Ozanne et al. 2006). Generally, during the EMT, epithelial cells become spindle shaped and genes such as that encoding E-Cad are downregulated, creating mesenchymal cells (Cavallaro et al. 2002; Maeda et al. 2005). Transcriptional repressors including SNAI1, SLUG, ZEB1, and ZEB2 bind to the E-Cad promoter, inhibiting transcription (Koppikar et al. 2008). Several lines of evidence suggest that EMT-activating transcription factors, including SNAI1, SLUG, Twist1, and ZEB1, enhance glioblastoma proliferation, invasion, and migration (Han et al. 2011; Mahabir et al. 2014; Mikheeva et al. 2010; Xia et al. 2010; Yang et al. 2010).

We hypothesized that the most critical factor affecting the EMT in terms of glioma invasion would be evident in highly invasive hypermotile cells. On induction of hypermotility via repetitive monolayer scratching, the levels of most EMT markers increased at both the mRNA and protein levels (N-Cad, SLUG, Twist1, and FN), in line with the findings of previous reports; invasion and migration were enhanced upon induction of the EMT in glioma cells (Han et al. 2011; Mikheeva et al. 2010; Xia et al. 2010; Yang et al. 2010). We used IHC to explore the similar (but not identical) roles played by various factors. SLUG was differentially expressed by tumor region (i.e., less in the center; more at the peripheral infiltrating margins), but SNAI1 and Twist1 were not. This SLUG expression pattern was evident in both mice with

patient-derived glioblastoma xenografts and human glioblastoma samples. Thus, SLUG may be important in invasion by infiltrating glioma margins. The biological significance of infiltration is acute for malignant gliomas; incomplete resection is unavoidable and residual tumor cells cause treatment failure and tumor recurrence. Yang et al. found that SLUG was a prime invasion-related transcription factor, as revealed by analysis of genome-wide mRNA expression by human glioblastoma (Yang et al. 2010).

The EMT imparts stem-like properties to cancer cells. Stemness is the ability of a cell to perpetuate its lineage in an asymmetric manner, giving rise to differentiated cells on the one hand but maintaining a stem cell identity on the other (Aponte and Caicedo 2017). Cancer stem cells may drive cancer progression, associated with rapid growth, invasion, metastasis, and recurrence (Aponte and Caicedo 2017). Induction of the EMT promoted stem-like properties in cancer cells, which exhibited a mesenchymal phenotype and increased plasticity (Mani et al. 2008; May et al. 2011). Here, we found that induction of EMT factors in hypermotile cells enhanced stemness. In such cells, expression of the stemness markers CD133, Eph- B1, CD44, ALDH1, HES1, and Msi increased, as did the neurosphere-forming capacity. Additionally, genetic modulation of SLUG expression may explain the therapeutic resistance of malignant glioma cells. SLUG-overexpressing cells exhibited an enhanced colony-forming ability after irradiation, and SLUG-knockdown cells a reduced capacity. SLUG-overexpressing cells were resistant to TMZ. The mesenchymal phenotype and stemness conferred resistance to chemoradiotherapy.

Cancer cells expressing E-Cad are more sensitive to chemotherapeutic drugs than cells exhibiting the mesenchymal phenotype (Fuchs et al. 2008; Li et al. 2009; Witta et al. 2006; Yang et al. 2006). Loss of E-Cad expression is a hallmark of the EMT and cancer metastases; E-Cad is one of the first SLUG targets (Bolos et al. 2003; Hajra et al. 2002). Glial cells (derived from the neuroepithelial crest) do not express E-Cad; the conventional 'E-Cad to N-Cad switch' is unlikely to be a feature of malignant gliomas (Utsuki et al. 2002). Rather than referring to the EMT of epithelial malignancy, consideration of a glial-to-mesenchymal transition may be more appropriate (Mahabir et al. 2014). Regardless of the term used to describe the phenomenon, enhancement of the mesenchymal phenotype is frequently observed in gliomas. SLUG induces chemotherapeutic resistance by repressing self-renewal genes such as NANOG, HDAC1, and TCF4, leading to the acquisition of a stem cell-like phenotype and thus enhancing the numbers of drug-resistant cells (Kurrey et al. 2009). $SLUG^{-/-}$ mice were markedly more radiosensitive than wild-type mice (Inoue et al. 2002). The EMT and cancer stemness may explain both therapeutic resistance and invasiveness, the two biggest obstacles in malignant glioma treatment.

We evaluated SLUG expression both in our cohort and the larger REMBRANDT cohort. Using the WHO classification, high-intensity SLUG expression was frequently observed in high-grade gliomas. SLUG levels correlated with glioma histological grade in a previous study similarly (Yang et al. 2010). Although downregulated SLUG did not afford an OS benefit, a survival advantage in terms of PFS was observed in our patients exhibiting low-level SLUG expression. The REMBRANDT data confirmed the clinical importance of SLUG expression in the OS context. As an EMT factor, SLUG seems to play an important role in terms of prognosis of glioma patient. Patients whose tumor samples were subjected to RNA-Seq analysis underwent chemoradiotherapy, and all recurrent tumors exhibited increased SLUG expression. Based on TCGA data analysis, mRNA level of SLUG in recurrent glioblastoma samples was significantly higher than the initial samples. Similarly, a recent study sought a multi-cancer, mesenchymal transition gene expression signature in data from TCGA, and linked a low-level EMT signature to prolonged PFS (Cheng et al. 2012). The human TMZ-resistant cell lines T98G and LN18 exhibited increased SLUG expression compared to the parental cells. Also, in mice orthotopically implanted with GL261, SLUG expression increased after TMZ treatment. Kubelt et al. earlier reported that the levels of mRNAs encoding various EMT markers increased after addition of TMZ (Kubelt et al. 2015). The cited authors did not correlate clinical information (a history of chemoradiation) with EMT marker levels in paired primary and recurrent gliomas. However, when T98G glioma cells were exposed to TMZ, markers of the EMT were induced, consistent with the increased SLUG expression evident in recurrent human glioma tissues and TMZ-resistant cell lines (Kubelt et al. 2015).

The SNAI1 family is composed of three members: SNAI1 (SNAIL), SNAI2 (SLUG), and SNAI3 (SMUC); all contain a single C-terminal zinc finger cluster that binds to E-boxes in the regulatory regions of target genes (Barrallo-Gimeno and Nieto 2005). Particularly in malignant glioma, SNAI1 has been shown to contribute to the radiation-induced mesenchymal transition. In a previous study, SNAI1 exhibited a sustained response to radiation, and the levels of other EMT regulators (SLUG and Twist1) increased to some extent (Mahabir et al. 2014). We hypothesize that the EMT regulators function co-operatively during the development of glioma recurrence, but that their roles differ spatiotemporally. For example, SLUG may drive the invasive phenotype at tumor-infiltrating margins and SNAI1 may precipitate the mesenchymal transition after irradiation, although the contributions made by both proteins tend to be synergistic in terms of resistance to chemoradiotherapy. In other aspects, Twist1 acts predominantly to induce transformation from glioblastoma to gliosarcoma, more aggressive and

intractable variant despite all kinds of therapy (Nagaishi et al. 2012; Nordfors et al. 2015).

However, further investigation needs to be performed to reveal the mechanistic links between SLUG and cancer stemness markers or key parameters for new 2016 WHO glioma classification, such as IDH1 mutation, 1p/19q co-deletion, or MGMT promoter methylation (Louis et al. 2016).

Conclusions

We found that SLUG is involved in the regulation of glioma invasion at the infiltrating tumor margins, and may also be involved in the development of therapeutic resistance and glioma recurrence. As recurrent tumors developing after chemoradiation tend to display mesenchymal phenotypes, current therapies may need to be refined by reference to tumor evolution. SLUG can be targeted during treatment, to reduce or halt initial invasion and recurrence.

Acknowledgements The English in this document has been checked by at least two professional editors, both native speakers of English. For a certificate, please see: http://www.textcheck.com/certificate/T7CJ5c.

Author contributions KHL and KSM designed this study. SJO, OK, and EJA carried out the experiment. SJO, KHL, and KSM drafted the manuscript. DK, TYJ, SJ, EHK, and JHL collected clinical data. JHL and KHL carried out pathological examination. KHL, EHK, and KSM carried out the statistical analysis. DK, KKK, and HK assisted with the manuscript preparation and data analysis. All authors read and approved the final manuscript.

Funding This work was supported by Basic Science Research Program through the National Research Foundation of Korea (NRF) funded by the Ministry Grant 2016R1A2B1014597 (KHL) and 2016R1C1B2007494 (KSM), partly by Chonnam National University Hospital Biomedical Research Institute Grant HCRI17902-21 (KSM). There was no role of the funding bodies in the design of the study, in the collection, analysis, and interpretation of data or in writing the manuscript.

Data availability The datasets used and analyzed during the current study are available from the corresponding author on reasonable request.

Competing interest The authors declare that they have no competing interests.

Ethics approval The Chonnam National University Hwasun Hospital Institutional Review Board approved this study (CNUHH-2016-081). We obtained written informed consent from patients or their legal surrogates for our use of resected glioma samples.

References

Aponte PM, Caicedo A (2017) Stemness in cancer: stem cells, cancer stem cells, and their microenvironment. Stem Cells Int 2017:5619472. https://doi.org/10.1155/2017/5619472

Barrallo-Gimeno A, Nieto MA (2005) The Snail genes as inducers of cell movement and survival: implications in development and cancer. Development 132:3151–3161. https://doi.org/10.1242/dev.01907

Bolos V, Peinado H, Perez-Moreno MA, Fraga MF, Esteller M, Cano A (2003) The transcription factor Slug represses E-cadherin expression and induces epithelial to mesenchymal transitions: a comparison with Snail and E47 repressors. J Cell Sci 116:499–511

Cano A et al (2000) The transcription factor snail controls epithelial-mesenchymal transitions by repressing E-cadherin expression. Nat Cell Biol 2:76–83. https://doi.org/10.1038/35000025

Cavallaro U, Schaffhauser B, Christofori G (2002) Cadherins and the tumour progression: is it all in a switch? Cancer Lett 176:123–128

Cheng WY, Kandel JJ, Yamashiro DJ, Canoll P, Anastassiou D (2012) A multi-cancer mesenchymal transition gene expression signature is associated with prolonged time to recurrence in glioblastoma. PLoS ONE 7:e34705. https://doi.org/10.1371/journal.pone.0034705

Dang H, Ding W, Emerson D, Rountree CB (2011) Snail1 induces epithelial-to-mesenchymal transition and tumor initiating stem cell characteristics. BMC Cancer 11:396. https://doi.org/10.1186/1471-2407-11-396

Fuchs BC, Fujii T, Dorfman JD, Goodwin JM, Zhu AX, Lanuti M, Tanabe KK (2008) Epithelial-to-mesenchymal transition and integrin-linked kinase mediate sensitivity to epidermal growth factor receptor inhibition in human hepatoma cells. Cancer Res 68:2391–2399. https://doi.org/10.1158/0008-5472.CAN-07-2460

Gonzalez DM, Medici D (2014) Signaling mechanisms of the epithelial-mesenchymal transition. Sci Signal 7:re8. https://doi.org/10.1126/scisignal.2005189

Gupta GP, Massague J (2006) Cancer metastasis: building a framework. Cell 127:679–695. https://doi.org/10.1016/j.cell.2006.11.001

Hajra KM, Chen DY, Fearon ER (2002) The SLUG zinc-finger protein represses E-cadherin in breast cancer. Cancer Res 62:1613–1618

Han SP et al (2011) SNAI1 is involved in the proliferation and migration of glioblastoma cells. Cell Mol Neurobiol 31:489–496. https://doi.org/10.1007/s10571-010-9643-4

Inoue A et al (2002) Slug, a highly conserved zinc finger transcriptional repressor, protects hematopoietic progenitor cells from radiation-induced apoptosis in vivo. Cancer Cell 2:279–288

Kalluri R, Neilson EG (2003) Epithelial-mesenchymal transition and its implications for fibrosis. J Clin Invest 112:1776–1784. https://doi.org/10.1172/Jci200320530

Kleihues P, Louis DN, Wiestler OD, Burger PC, Scheithauer BW (2007) WHO grading of tumours of the central nervous system In: Bosman FT, Jaffe ES, Lakhani SR, Ohgaki H (eds) WHO classification of tumours of the central nervous system. World Health Organization classification of tumours, 4th edn. International Agency for Research on Cancer, Lyon

Koppikar P et al (2008) Constitutive activation of signal transducer and activator of transcription 5 contributes to tumor growth, epithelial-mesenchymal transition, and resistance to epidermal growth factor receptor targeting. Clin Cancer Res 14:7682–7690. https://doi.org/10.1158/1078-0432.CCR-08-1328

Kubelt C, Hattermann K, Sebens S, Mehdorn HM, Held-Feindt J (2015) Epithelial-to-mesenchymal transition in paired human primary and recurrent glioblastomas. Int J Oncol 46:2515–2525

Kurrey NK, Amit K, Bapat SA (2005) Snail and Slug are major determinants of ovarian cancer invasiveness at the transcription level. Gynecol Oncol 97:155–165. https://doi.org/10.1016/j.ygyno.2004.12.043

Kurrey NK, Jalgaonkar SP, Joglekar AV, Ghanate AD, Chaskar PD, Doiphode RY, Bapat SA (2009) Snail and slug mediate radioresistance and chemoresistance by antagonizing p53-mediated apoptosis and acquiring a stem-like phenotype in ovarian cancer cells. Stem Cells 27:2059–2068. https://doi.org/10.1002/stem.154

Kwon SM et al (2015) Recurrent glioblastomas reveal molecular subtypes associated with mechanistic implications of drug-resistance. PLoS ONE 10:e0140528. https://doi.org/10.1371/journal.pone.0140528

Lee KH et al (2015) KITENIN promotes glioma invasiveness and progression, associated with the induction of EMT and stemness markers. Oncotarget 6:3240–3253. https://doi.org/10.18632/oncotarget.3087

Li Y, VandenBoom TG 2nd, Kong D, Wang Z, Ali S, Philip PA, Sarkar FH (2009) Up-regulation of miR-200 and let-7 by natural agents leads to the reversal of epithelial-to-mesenchymal transition in gemcitabine-resistant pancreatic cancer cells. Cancer Res 69:6704–6712. https://doi.org/10.1158/0008-5472.CAN-09-1298

Louis DN, Hiroko O, Wiestler OD, Cavenee WK, Ellison DW (2016) WHO Classification of tumours of the central nervous system, vol 1. International Agency for Research on Cancer, Lyon

Maeda M, Johnson KR, Wheelock MJ (2005) Cadherin switching: essential for behavioral but not morphological changes during an epithelium-to-mesenchyme transition. J Cell Sci 118:873–887. https://doi.org/10.1242/jcs.01634

Mahabir R et al (2014) Sustained elevation of Snail promotes glial-mesenchymal transition after irradiation in malignant glioma. Neuro Oncol 16:671–685. https://doi.org/10.1093/neuonc/not239

Mani SA et al (2008) The epithelial-mesenchymal transition generates cells with properties of stem cells. Cell 133:704–715. https://doi.org/10.1016/j.cell.2008.03.027

May CD, Sphyris N, Evans KW, Werden SJ, Guo W, Mani SA (2011) Epithelial-mesenchymal transition and cancer stem cells: a dangerously dynamic duo in breast cancer progression. Breast Cancer Res 13:202. https://doi.org/10.1186/bcr2789

Mikheeva SA et al (2010) TWIST1 promotes invasion through mesenchymal change in human glioblastoma. Mol Cancer 9:194. https://doi.org/10.1186/1476-4598-9-194

Nagaishi M et al (2012) Transcriptional factors for epithelial-mesenchymal transition are associated with mesenchymal differentiation in gliosarcoma. Brain Pathol 22:670–676. https://doi.org/10.1111/j.1750-3639.2012.00571.x

Nieto MA (2002) The snail superfamily of zinc-finger transcription factors. Nat Rev Mol Cell Biol 3:155–166. https://doi.org/10.1038/nrm757

Nieto MA (2011) The ins and outs of the epithelial to mesenchymal transition in health and disease. Annu Rev Cell Dev Biol 27:347–376. https://doi.org/10.1146/annurev-cellbio-092910-154036

Noh MG et al (2017) Prognostic significance of E-cadherin and N-cadherin expression in Gliomas. BMC Cancer 17:583. https://doi.org/10.1186/s12885-017-3591-z

Nordfors K et al (2015) Twist predicts poor outcome of patients with astrocytic glioma. J Clin Pathol 68:905–912. https://doi.org/10.1136/jclinpath-2015-202868

Ozanne BW, Spence HJ, McGarry LC, Hennigan RF (2006) Invasion is a genetic program regulated by transcription factors. Curr Opin Genet Dev 16:65–70. https://doi.org/10.1016/j.gde.2005.12.012

Peinado H, Olmeda D, Cano A (2007) Snail, Zeb and bHLH factors in tumour progression: an alliance against the epithelial phenotype? Nat Rev Cancer 7:415–428. https://doi.org/10.1038/nrc2131

Polyak K, Weinberg RA (2009) Transitions between epithelial and mesenchymal states: acquisition of malignant and stem cell traits. Nat Rev Cancer 9:265–273. https://doi.org/10.1038/nrc2620

Savagner P, Yamada KM, Thiery JP (1997) The zinc-finger protein slug causes desmosome dissociation, an initial and necessary step for growth factor-induced epithelial-mesenchymal transition. J Cell Biol 137:1403–1419. https://doi.org/10.1083/jcb.137.6.1403

Shih JY et al (2005) Transcription repressor Slug promotes carcinoma invasion and predicts outcome of patients with lung adenocarcinoma. Clin Cancer Res 11:8070–8078. https://doi.org/10.1158/1078-0432.CCR-05-0687

Shioiri M et al (2006) Slug expression is an independent prognostic parameter for poor survival in colorectal carcinoma patients. Br J Cancer 94:1816–1822. https://doi.org/10.1038/sj.bjc.6603193

Singh A, Settleman J (2010) EMT, cancer stem cells and drug resistance: an emerging axis of evil in the war on cancer. Oncogene 29:4741–4751. https://doi.org/10.1038/onc.2010.215

Uchikado Y, Natsugoe S, Okumura H, Setoyama T, Matsumoto M, Ishigami S, Aikou T (2005) Slug expression in the E-cadherin preserved tumors is related to prognosis in patients with Esophageal squamous cell carcinoma. Clin Cancer Res 11:1174–1180

Utsuki S, Sato Y, Oka H, Tsuchiya B, Suzuki S, Fujii K (2002) Relationship between the expression of E-, N-cadherins and beta-catenin and tumor grade in astrocytomas. J Neuro-oncol 57:187–192

Wellner U et al (2009) The EMT-activator ZEB1 promotes tumorigenicity by repressing stemness-inhibiting microRNAs. Nat Cell Biol 11:1487–1495. https://doi.org/10.1038/ncb1998

Witta SE et al (2006) Restoring E-cadherin expression increases sensitivity to epidermal growth factor receptor inhibitors in lung cancer cell lines. Cancer Res 66:944–950. https://doi.org/10.1158/0008-5472.CAN-05-1988

Xia M, Hu MH, Wang J, Xu YJ, Chen XB, Ma YD, Su L (2010) Identification of the role of Smad interacting protein 1 (SIP1) in glioma. J Neuro-oncol 97:225–232. https://doi.org/10.1007/s11060-009-0015-1

Yang AD et al (2006) Chronic oxaliplatin resistance induces epithelial-to-mesenchymal transition in colorectal cancer cell lines. Clin Cancer Res 12:4147–4153. https://doi.org/10.1158/1078-0432.CCR-06-0038

Yang HW, Menon LG, Black PM, Carroll RS, Johnson MD (2010) SNAI2/Slug promotes growth and invasion in human gliomas. BMC Cancer 10:301. https://doi.org/10.1186/1471-2407-10-301

Affiliations

Se-Jeong Oh[1,2] · Eun-Jung Ahn[1,2] · Ok Kim[2] · Daru Kim[2] · Tae-Young Jung[1] · Shin Jung[1] · Jae-Hyuk Lee[2] · Kyung-Keun Kim[3] · Hangun Kim[4] · Eui Hyun Kim[5] · Kyung-Hwa Lee[2] · Kyung-Sub Moon[1]

Se-Jeong Oh
ddalki7598@hanmail.net

Eun-Jung Ahn
happybear33@naver.com

Ok Kim
oasis99k@hanmail.net

Daru Kim
kingdaru@hanmail.net

Tae-Young Jung
jung-ty@chonnam.ac.kr

Shin Jung
sjung@chonnam.ac.kr

Jae-Hyuk Lee
jhlee@jnu.ac.kr

Kyung-Keun Kim
kimkk@chonnam.ac.kr

Hangun Kim
hangunkim@sunchon.ac.kr

Eui Hyun Kim
euihyunkim@yuhs.ac

[1] Department of Neurosurgery, Chonnam National University Research Institute of Medical Science, Chonnam National University Hwasun Hospital and Medical School, 322 Seoyang-ro, Hwasun-eup, Hwasun-gun, Jeollanam-do 58128, South Korea

[2] Department of Pathology, Chonnam National University Research Institute of Medical Science, Chonnam National University Hwasun Hospital and Medical School, 322 Seoyang-ro, Hwasun-eup, Hwasun-gun, Jeollanam-do 58128, South Korea

[3] Medical Research Center of Gene Regulation and Center for Creative Biomedical Scientists, Chonnam National University Medical School, Gwangju, South Korea

[4] College of Pharmacy and Research Institute of Life and Pharmaceutical Sciences, Sunchon National University, Sunchon, Jeollanam-do, South Korea

[5] Department of Neurosurgery, Severance Hospital, Yonsei University College of Medicine, Seoul, South Korea